

Fast Proton Titration Scheme for Multiscale Modeling of Protein Solutions

Andre Azevedo Reis Teixeira,[†] Mikael Lund,[‡] and Fernando Luís Barroso da Silva^{*,†,‡}

Department of Physics and Chemistry, 14040-903 Av. do café, s/no., FCFRP—USP, Ribeirão Preto, SP, Brazil, Department of Theoretical Chemistry Chemical Center, Lund University, P.O. Box 124-S-221 00, Lund, Sweden, and Department of Physics and Chemistry, 14040-903 Av. do café, s/no., FCFRP—USP, Ribeirão Preto, SP, Brazil

Received June 7, 2010

Abstract: Proton exchange between titratable amino acid residues and the surrounding solution gives rise to exciting electric processes in proteins. We present a proton titration scheme for studying acid–base equilibria in Metropolis Monte Carlo simulations where salt is treated at the Debye–Hückel level. The method, rooted in the Kirkwood model of impenetrable spheres, is applied on the three milk proteins α -lactalbumin, β -lactoglobulin, and lactoferrin, for which we investigate the net-charge, molecular dipole moment, and charge capacitance. Over a wide range of pH and salt conditions, excellent agreement is found with more elaborate simulations where salt is explicitly included. The implicit salt scheme is orders of magnitude faster than the explicit analog and allows for transparent interpretation of physical mechanisms. It is shown how the method can be expanded to multiscale modeling of aqueous salt solutions of many biomolecules with nonstatic charge distributions. Important examples are protein–protein aggregation, protein–polyelectrolyte complexation, and protein–membrane association.

1. Introduction

Electrostatic interactions are crucial for biological^{1–3} and technological phenomena involving proteins. Examples are protein foams in the food industry,⁴ food and pharmaceutical formulations,^{5,6} enzyme immobilization,⁷ protein separation, and other bioprocesses.^{8–11} These interactions are directly related to a multitude of ionized amino acid residues: aspartic acid, glutamic acid, cysteine not involved in SS bonds, tyrosine, C-terminal, arginine, histidine, lysine, and N-terminal. Consequently, salt and pH have a significant effect on protein solution behavior, and a wealth of studies of electrostatic interactions in and between biomolecules is available.^{1–3,12–14}

The tendency of amino acids to change their ionization states due to an external electrostatic perturbation is directly related to the charge fluctuation of the protein—the so-called

protein charge capacitance, C .¹² This fluctuation, quantified by C , is responsible for an important purely electrostatic attractive interaction observed in several systems.^{13–21} While the *charge regulation* mechanism has been known for a long time,^{22,23} only recently has it become possible to accurately extract C from the three-dimensional protein structure.

In many practical applications the molar concentration of salt is relatively high—100 mM or more—which invariably increases the computation time of any continuum electrostatic model that incorporates salt particles *explicitly*. The situation becomes even worse in the case of low protein concentrations. In such studies, often the main focus is not on the salt particles themselves but rather on their effect on the interactions between the proteins or biopolymers. Since many practical experimental conditions are not far from the isoelectric point (pI), the electrostatic coupling²⁴ tends to be small, and salt can be treated at the Debye–Hückel level.^{25–27}

Monte Carlo (MC) titration schemes using explicit ions have been successfully applied to describe ionization equilibria and protein complexation.^{12,28–31} Titrating MC simulations have also been used to study the impact of the charge

* To whom correspondence should be addressed. Tel.: +55 (16)3602 42 19. Fax: +55 (16)3602 48 80. E-mail: fernando@fcfrp.usp.br.

[†] Department of Physics and Chemistry, FCFRP—USP.

[‡] University of Lund.

Table 1. Details of the Three Studied Proteins^a

protein	PDB	residues	radius (Å)	mass (kDa)
α -LA	1F6S (A)	122	18	14
β -LG	1BEB (A+B)	312	24	35
LF	1BLF	685	30	76

^a The radius is that of a sphere with the same volume as the three dimensional structure of the protein.

regulation mechanism mentioned above.^{12–14} In these approaches the explicit inclusion of ions requires excessive computational resources at conditions where the salt concentration is high when at the same time the protein concentration is low.

The Poisson–Boltzmann (PB) approximation has been widely used for protein electrostatics, ranging from the early Tanford–Kirkwood model^{32,33} to advanced finite element methods where boundary conditions are numerically matched on the anisotropic protein surface.³⁴ For studying many proteins, a fairly simple approach is required, while maintaining the essential physics. In this work, we present a fast algorithm for proton titration in Metropolis Monte Carlo simulations where salt is treated implicitly. This drastically reduces the computation time while capturing the main effects of pH and salt.

Milk proteins have diverse physicochemical properties and extensive applications within formulation technology in the pharmaceutical and food industries.^{20,35,36} They are further used as model systems for biophysical studies,^{37,38} and their electrostatic properties are hence of considerable interest. In this study, we use α -lactalbumin (α -LA), β -lactoglobulin (β -LG), and lactoferrin (LF) as test cases for our theoretical models. The properties and structures of all three proteins are listed and shown in Table 1 and Figure 1, respectively, and we now briefly introduce each protein:

The globular 14 kDa protein α -LA is part of the C-type lysozyme family and corresponds to approximately 20% of the proteins present in bovine milk serum. α -LA acts as an enzyme for the biosynthesis of lactose,³⁵ and the tertiary structure is available at 2.2 Å resolution.³⁹

β -LG is the main protein constituent of bovine milk serum, corresponding to roughly 50%. In mammalian animals, it has two main functions: binding of retinol (vitamin A) and stimulating lipolysis. Under normal milk conditions, β -LG is found in a dimer/monomer equilibrium which is shifted toward the dimer as the pH approaches pI. We here study the dimeric form since its high molecular dipole moment³⁵ provides a more challenging case for the theoretical models. The used tertiary structure (a mixture of two genetic variants) was obtained by X-ray diffraction with a 1.8 Å resolution.⁴⁰

With its molecular mass of 76 kDa, LF is the largest protein studied. LF is a bacteriostatic agent that sequesters iron ions. Commercial applications are many, including nutraceuticals production, antioxidant agents, and oral care products. The tertiary structure of LF is available at 2.8 Å resolution, and contrary to the previous proteins that have pI values between 4.2 to 5.4, the pI \approx 9 of LF is on the basic side.³⁵

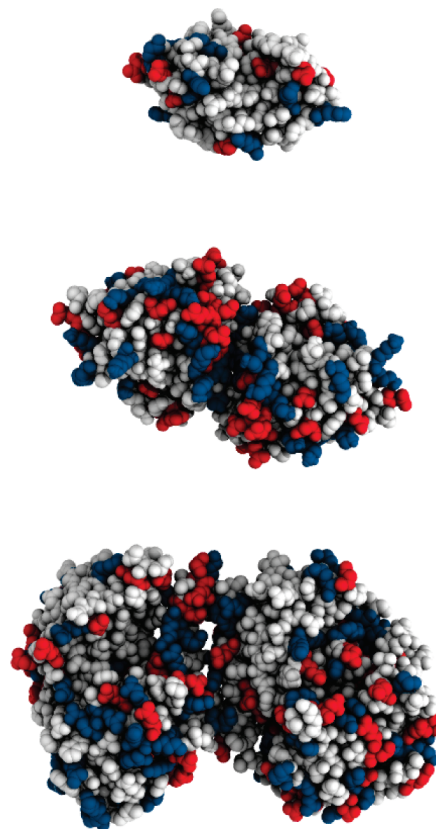


Figure 1. Structures of the three studied milk proteins. Acidic and basic residues are shown in red and blue, respectively. From top to bottom: α -LA (PDB ID: 1F6S), β -LG (PDB ID: 1BEB), and LF (PDB ID: 1BLF).

2. Models and Theory

2.1. Titration Behavior at Ideal Conditions. In this section, we describe general equilibrium properties of weak acids which shall serve as a foundation for the two MC titration schemes presented later. We start with the dissociation process for a monoprotic acid



with the corresponding thermodynamic equilibrium constant

$$K_a = \frac{\gamma_{\text{H}^+} \gamma_{\text{A}^-}}{\gamma_{\text{HA}}} \times \frac{c_{\text{H}^+} c_{\text{A}^-}}{c_{\text{HA}}} \quad (1)$$

where γ and c are activity coefficients and concentrations, respectively. It then follows that the free energy difference between the protonated and deprotonated form is

$$\beta \Delta A_{\text{HA} \rightarrow \text{A}^-} = -\ln \frac{c_{\text{A}^-}}{c_{\text{HA}}} = -\ln \frac{\gamma_{\text{A}^-}}{\gamma_{\text{HA}}} - (\text{pH} - \text{p}K_a) \ln 10 \quad (2)$$

where $\beta = 1/k_B T$ is the inverse thermal energy and $\text{pH} = -\log(c_{\text{H}^+} \gamma_{\text{H}^+})$. We now choose a reference state so that at infinite dilution, $\gamma \rightarrow 1$ and the degree of dissociation can hence be written as

$$\alpha(\text{pH}) = \frac{c_{\text{A}^-}}{c_{\text{HA}} + c_{\text{A}^-}} = \frac{10^{\text{pH} - \text{p}K_a}}{1 + 10^{\text{pH} - \text{p}K_a}} \quad (3)$$

If for a protein with many titratable groups, we (briefly!) assume that each residue is unaffected by the rest, the average net-charge number of the protein, Z_p , can be estimated by summing over all N_{acid} acidic and N_{basic} basic residues, requiring only the primary structure

$$Z_p(\text{pH}) = \sum_{i=1}^{N_{\text{basic}}} [1 - \alpha_i(\text{pH})] - \sum_{i=1}^{N_{\text{acid}}} \alpha_i(\text{pH}) \quad (4)$$

Due to proton exchange with the surrounding solution, the charge state of ionizable groups will *fluctuate* over time. This fluctuation leads to the charge regulation mechanism^{23,41,42} and can be defined as a capacitance¹²

$$C = \langle Z_p^2 \rangle - \langle Z_p \rangle^2 = -\frac{1}{\ln 10} \times \frac{\partial Z_p}{\partial \text{pH}} \quad (5)$$

where the brackets denote statistical mechanical ensemble averages. Hence, C can be obtained simply by differentiating eq 4 with respect to pH.

Naturally, two proteins with the same amino acid composition have identical charge and capacitance at all pH values if ideal behavior is assumed. That is, neglecting intra- and intermolecular interactions ($\gamma \rightarrow 1$) precludes any distinction between different conformations of the same molecule. Nevertheless, the ideal contribution to the net charge and capacitance is a useful first approximation, and by comparing with full titration and capacitance data, we can deduce the effects of the tertiary structure and surrounding salt. Further, at high salt concentrations, electrostatic interactions are screened, and experimental data approach the ideal case.⁴³

2.2. Proton Titration with Explicit Salt. The Monte Carlo (MC) Metropolis algorithm^{44–46} is a stochastic method based on random walks in coordinate space where each configuration has a statistical weight defined by the Boltzmann distribution.^{25,45,46} Within the primitive model of electrolytes, macromolecular titration behavior has previously been studied using MC simulations,^{31,47,48} and we here rely on the following procedure: A single, rigid protein is placed at the center of a spherical simulation cell that also encapsulates mobile ions (counterions and added salt), see Figure 2. The protein is described in mesoscopic detail so that the full, experimentally determined structure is replaced by a coarse grained representation where each amino acid is represented by a sphere.⁴⁹ Except where otherwise stated, proteins are used in their monomeric form (first structure if more present in PDB). Mobile ions and amino acid residues are described by hard spheres of diameter σ_i and charge $q_i = z_i e$, where e is the elementary charge and z_i is the valency. Any two particles, i and j , in the system interact via a solvent-mediated Coulomb potential, augmented by a repulsive hard sphere term, i.e., the primitive model of electrolytes²⁵

$$u^{\text{el}}(r_{ij}) = \begin{cases} \infty, & r_{ij} \leq (\sigma_i + \sigma_j)/2 \\ \frac{e^2 z_i z_j}{4\pi\epsilon_0 \epsilon_r r_{ij}}, & \text{otherwise} \end{cases} \quad (6)$$

where ϵ_0 is the permittivity of vacuum ($\epsilon_0 = 8.854 \times 10^{-12}$ C²/Nm²), $\epsilon_r = 78.7$ is the relative dielectric constant of water,

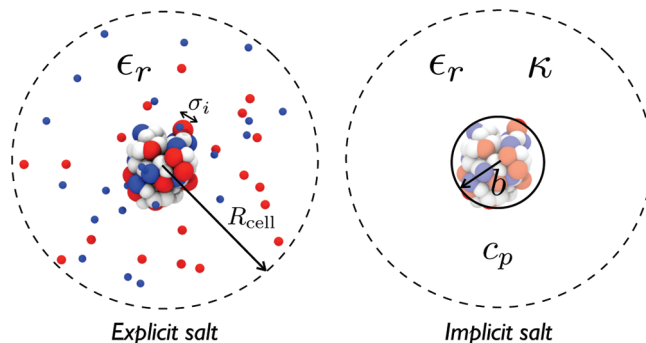


Figure 2. Schematic representation of the Monte Carlo simulation schemes. Left: Amino acids, salt, and counterions are described by (charged) hard spheres of diameter σ_i . Concentrations of salt, protein, and counterions are determined by the radius of the simulation cell, R_{cell} . Right: Salt is implicitly accounted for by the inverse Debye screening length, κ , which also varies with the counterion concentration and hence the protein concentration, c_p . The volume of the salt-free region defined by the sphere b matches that of the protein.

Table 2. Intrinsic pK_a Values for Titratable Amino Acid Groups⁵⁰

	Asp	Glu	Cys ^a	Tyr	Ctr	Arg	His	Lys	Ntr
pK_a	4.0	4.4	9.5	9.6	3.8	12.0	6.3	10.4	7.5

^a Only cysteins not engaged in sulfide bridges can titrate.

and $T = 298.15$ K is the temperature. During the MC simulation, mobile ions ($\sigma_{\pm} = 4$ Å) are allowed to translate in any direction while the charges on the protein fluctuate according to the following semicanonical MC move:

1. A titratable site on the protein is chosen by random.
2. If deprotonated, move the charge from the bulk solution to the site (protonation process). If protonated, move the proton to the bulk solution (deprotonation process). Note that no new particle is introduced into the dense protein environment. The proton binding site is already there, given by the experimental structure, and we merely increase (or decrease) its charge by +1.
3. The move is accepted with the probability,

$$\min(1, e^{-\beta \Delta U_{\text{el}} \pm (\text{pH} - \text{pK}_a) \ln 10}) \quad (7)$$

where ΔU_{el} is the change in total electrostatic energy, calculated by summing over all particles before and after the move according to eq 6. The second term in the exponential accounts for the free energy change of the (de)protonation process for a single amino acid, not affected by the presence of the rest of the protein nor by salt (see eq 2). The magnitude of this term is determined by pH and the intrinsic pK_a value. The latter is a measured property which *implicitly* includes nonelectrostatic interactions (dispersion, solvation effects, polarization, etc.) that are not explicitly accounted for in the MC Hamiltonian. In this work, we employ pK_a values given by Nozaki and Tanford,⁵⁰ see Table 2.

In summary, the MC simulation enables us to calculate statistical mechanical ensemble averages, integrated over all salt positions ($\mathbf{r}_i^{N_s}$) and protonation states (λ^{N_p})

$$\langle x \rangle = \frac{\int \int x(\mathbf{r}^{N_s}, \lambda^{N_p}) e^{-\beta U(\mathbf{r}^{N_s}, \lambda^{N_p})} d\mathbf{r}^{N_s} d\lambda^{N_p}}{\int \int e^{-\beta U(\mathbf{r}^{N_s}, \lambda^{N_p})} d\mathbf{r}^{N_s} d\lambda^{N_p}} \quad (8)$$

Important examples are the protein net charge, $\langle Z_p \rangle$; the molecular dipole moment, $\langle \mu \rangle$; and the capacitance, C .

An intense debate about the protein dielectric constant can be seen in the literature.^{51–56} In the presented scheme we assume a uniform dielectric constant for the entire system, including the protein. For a range of globular proteins, it has been shown that this approximation is indeed valid, mainly because most titratable sites are located at the surface and are thus well hydrated. In addition, a major part of any polarization contribution is implicitly included in the intrinsic pK_a values used. That is, we need only account for the *difference* in free energy between the residue in the protein and the reference model peptide for which the pK_a value was originally obtained. Unless the site is deeply buried, this difference will be small. For a detailed description of—perhaps surprisingly—*why* the uniform dielectric model works, the reader should consult ref 51.

2.3. Proton Titration with Implicit Salt. In the scheme described in the previous section, salt particles were explicitly included in the MC simulation. Here, we present a scheme for implicit salt titration based on Kirkwood's theory of impenetrable spheres.^{32,33} Consider a set of charges ez_1, \dots, ez_n distributed in a sphere of diameter σ_p immersed in a salt solution. The distance of closest approach between salt and the spherical macromolecule is defined by $b = (\sigma_p + \sigma_{\text{salt}})/2 \approx \sigma_p/2$. Assuming a uniform dielectric constant throughout the medium⁵¹ and neglecting higher-order multipolar terms for the salt–protein interactions, the free energy can be approximated by the leading terms in the Tanford–Kirkwood model,^{33,53}

$$w_{\text{ik}} \approx \frac{e^2}{4\pi\epsilon_0\epsilon_r} \left(\sum_{i>j}^n \frac{z_i z_j}{r_{ij}} - \frac{Z_p^2 \kappa}{2(1 + \kappa b)} \right) \quad (9)$$

where $Z_p = \sum_i^n z_i$, n is the number of protein ionizable sites, and κ is the inverse Debye screening length.^{57–59} Note that solvation free energies are implicitly accounted for by the intrinsic pK_a values, assuming that the residue is not deeply buried. The first term in eq 9 involves site–site interactions, while the second term accounts for all interactions with the surrounding salt.

For low ionic concentrations, it has been suggested^{60–62} that the concentration of counterions should be included in κ . We therefore employ the following definition of the screening length that includes both salt and counterions:

$$D = \kappa^{-1} = \sqrt{\frac{\epsilon_0 \epsilon_s k_B T}{2N_a e^2 I}} \quad (10)$$

where N_a is Avogadro's number, k_B is Boltzmann's constant ($k_B = 1.3807 \times 10^{-23} \text{ J} \cdot \text{K}^{-1}$), and T is the temperature. The ionic strength, I , is defined as,

$$I = \frac{1}{2} \sum_{i=1}^{N_{\text{ionic}}} c_i z_i^2 \quad (11)$$

where c_i is the molar concentration of species i and N_{ionic} is the total number of the ionic species (added salt particles and the counterions).

The MC protocol for implicit titration is similar to the one used for explicit salt in the previous section. The differences are that (1) salt particles and their MC moves are omitted and (2) the acceptance probability is

$$\min(1, e^{-\beta \Delta w_{\text{ik}} \pm (pH - pK_a) \ln 10}) \quad (12)$$

remembering that κ depends on the protonation state due to the inclusion of counterions in the ionic strength, c.f., eq 11. The new MC scheme is implemented in the Faunus package⁶³—a free, open-source framework for biomolecular simulation.

All Monte Carlo simulations—explicit and implicit salt alike—were performed with a protein concentration of 117.5 μM obtained through a cell radius of 150 Å. The salt concentration was varied between 5 and 150 mM. The protein structures were modeled in mesoscopic detail—i.e., each amino acid was treated as a single sphere.⁴⁹ Although this simplification greatly decreases the simulation time in explicit salt simulations, it has no effect with implicit salt—at least not for single protein systems. For the explicit and implicit salt models, typical simulation runs were carried out during the equilibration and production phases with 2×10^4 and 10^6 MC steps, respectively.

Finally, let us discuss a subtle difference between the two titration methods. In the case of explicit salt, charges literally move in and out of the bulk, and as such, ΔU_{el} in eq 7 accounts for the excess chemical potential of the protons. To satisfy eq 2, pH must be defined on the *concentration* scale, i.e., $pH^* = -\log c_{H^+}$. This double counting is absent from the implicit salt titration scheme where pH is correctly defined on the activity scale. It is however trivial to convert between the two scales via

$$pH = -\log(c_{H^+} \gamma_{H^+}) = pH^* - \log \gamma_{H^+} \quad (13)$$

In the presented explicit salt MC results, we estimate γ_{H^+} using the well-known Debye–Hückel expression²⁵ so as to transform to the *activity*-based pH scale. The maximum correction, needed at 150 mM salt, is less than 0.2 pH units.

3. Results and Discussion

In this section, we analyze and compare results obtained from the three different models: ideal (the analytical solution based on the amino acid composition), MC with explicit salt ions (the protocol with tertiary structures largely used in this field), and MC with the implicit salt description (the new scheme suggested here). Data are presented for the three whey proteins (α -LA, β -LG, and LF) at different pH and salt concentrations.

Protein Charge. We first investigate the effect of pH and salt on the protein net-charge number, $Z_p = \langle Z_p \rangle$. This is shown for α -LA, β -LG, and LF in Figure 3. In all cases, increasing the ionic strength tends to make the protein more charged, independent of the salt description. This is due to the reduced internal repulsion caused by salt screening, which pushes the titration curve closer to the ideal curve. This can

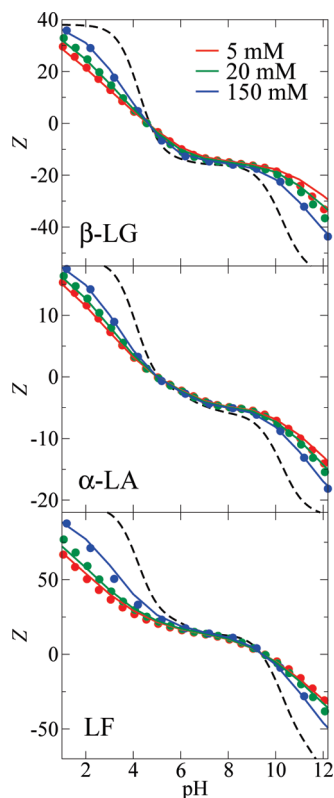


Figure 3. Net charges, Z_p , of the three proteins at different pH and salt concentrations. Calculated using explicit (symbols) and implicit (lines) salt MC simulations. The dashed lines represent the ideal titration curves—i.e., when no salt or intramolecular interactions are taken into account.

be understood from eq 9 by noting that when the salt concentration and hence κ become large, the second term approaches $Z_p^2/2b$, which is nothing but the self-energy of spreading Z_p on b . Neglecting multipolar terms, this self-energy approximately cancels out the first term whereby $\lim_{\kappa \rightarrow \infty} W_{\text{tk}} \approx 0$. This is in perfect agreement with experimental observations as demonstrated by the classical titration data for ribonuclease in KCl.⁴³ The agreement between the explicit and implicit schemes is very good. Even as the salt concentration is increased to 150 mM, one finds excellent agreement between the two MC procedures.

A weakness of the implicit salt model is that the isoelectric point, pI , is unaffected by the salt concentration since anisotropic protein–salt interactions are neglected in the truncated Kirkwood approach (eq 9). Nevertheless, explicit salt simulations—which account for *all* protein–salt interactions—do not reveal noticeable salt-dependent pI shifts for the three studied proteins. The calculated iso-electric points for the three proteins are 4.8, 5.4, and 9.7 for α -LA, β -LG, and (apo) LF, respectively. The corresponding experimental values are 4.2–4.5, 5.1, and 8.8.^{64,65} Despite its high affinity for iron, LF releases the iron ions from its binding sites below pH 6.0.⁶⁶ Differences between theoretical and experimental values for LF's pI have been observed before. Our MC data are in agreement with the theoretical value (9.4) reported by Steijns and van Hooijdonk.⁶⁷

Note also that in our model the protein structure is oblivious to pH changes. While this may be problematic at pH extremes, it is not a serious limitation at intermediate

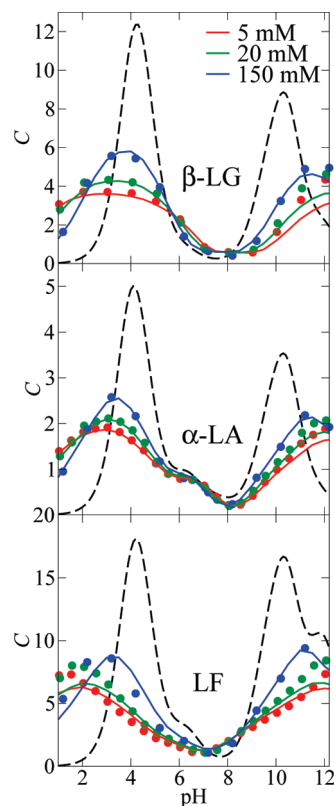


Figure 4. Electric capacitance, C , of the three proteins at different pH and salt concentrations, calculated using explicit (symbols) and implicit (lines) salt MC simulations. The dashed lines represent the ideal capacitance curves—i.e., when no salt or intramolecular interactions are taken into account.

pH values where the proteins are not subject to denaturation.⁶⁸ For mere comparison between explicit and implicit salt simulations, this is of course unimportant.

Protein Capacitance. Next, let us examine the protein charge capacitance, C —see eq 5. This property is important for macromolecular complexation as it quantifies charge regulation mechanisms.^{12,14,20,23} As C is a derivative, it is a more sensitive measure than the protein net charge. As can be seen in Figure 4, good agreement between the explicit and implicit salt descriptions is found—in particular for intermediate pH values where the net charge is relatively low. The peaks at high and low pH values are due to the large number of basic and acidic residues that titrate in these regions since proton fluctuations are maximized for $\text{pH} \approx \text{pK}_a$. Electrostatic interactions between titratable sites tend to lower and widen the capacitance peaks. This effect is well captured by both models, and when salt is added, we approach the ideal curve due to reasons already discussed.

Protein Dipole Moment. The molecular dipole moment, $\mu = |\sum_i^n r_i z_i|$, embodies the first step toward an arbitrary, anisotropic charge distribution. Since in the implicit titration model we treat protein–salt interactions as *isotropic*, we expect the dipole moment to be the hardest property to accurately reproduce. Yet, as can be seen in Figure 5, good agreement between the explicit and implicit model is found for α -LA and β -LG. LF, with dipole moments of up to 1600 D (interestingly at physiological pH), shows the largest discrepancies between the two models—especially at high

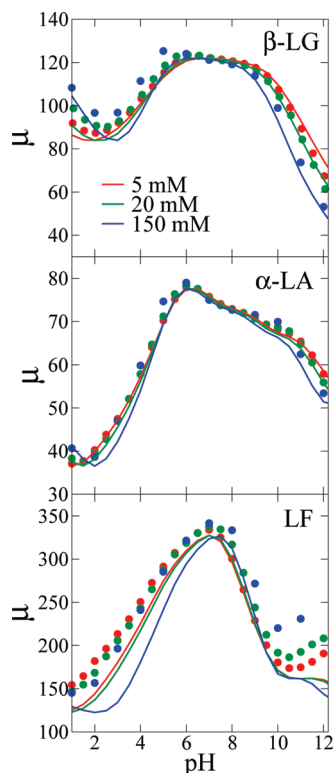


Figure 5. Molecular dipole moments, μ , of the three proteins at different pH and salt concentrations, calculated using explicit (symbols) and implicit (lines) salt MC simulations. The unit is electron $e \text{ \AA}$, which corresponds to 4.8 Debye (D).

and low pH values. LF deviates most from spherical symmetry, and it is expected that anisotropic protein–salt interactions play a larger role. As true also for the charge and capacitance, when $\text{pH} = \text{pI}$, the salt dependency disappears for the implicit titration scheme.

Many-Body Interactions. So far we have focused on protonation properties of single protein molecules in salt solutions. However, in the presence of other charged macromolecules,^{12,23} the protonation state may change. This perturbation can be captured by, for each proton move, evaluating the electrostatic interaction of the site with all *extra-molecular* charges in the system. The acceptance criteria then becomes

$$\min(1, e^{-\beta \Delta w_{ik} \pm (\text{pH} - \text{pK}_a) \ln 10 - \beta \Delta \sum \phi_i e z_i}) \quad (14)$$

where ϕ_i is the potential on i due to all external charges. Assuming that salt exclusion from the protein has only a minor effect on intermolecular interactions, we can approximate ϕ_i with a plain Debye–Hückel potential. Following this scheme, it is possible to introduce proton equilibria in many-body protein simulations at a minimal computational cost.

Performance. Lastly, we briefly discuss the computational performance of implicit versus explicit salt simulations. The computation time of an N -body simulation scales as N^2 , and explicit salt simulations hence decelerate for large salt concentrations when at the same time the protein concentration is low. This is illustrated in Figure 6, where we have plotted the number of salt particles per protein as a function

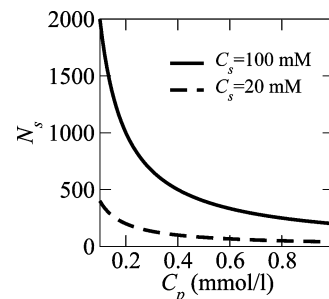


Figure 6. Number of salt particles, N_s , per protein plotted as a function of the protein concentration, C_p , for typical salt concentrations, C_s .

of the protein concentration. From this picture, it is clear that an implicit salt description leads to speed-ups of several orders of magnitude and that the computational time is independent of the salt concentration.

4. Conclusions

We present a Monte Carlo titration scheme within the Debye–Hückel implicit salt description. The model is tested against reference data obtained using explicit salt simulations for three different whey proteins in the concentration range 5–150 mM. The model very well reproduces electric properties such as net charge, dipole moment, and capacitance, even at relatively high ionic concentrations and in a wide span of pH values.

Elongated proteins show the largest deviations from the explicit salt results. This is explained by the fact that the implicit salt model neglects anisotropic salt–protein interactions and further assumes that salt exclusion from the protein is spherically symmetric. This becomes more evident at higher salt concentrations where the protein net charges tend to be larger.

Treating the salt implicitly drastically reduces the computation time and makes it independent of the ionic strength. Conversely, for explicit salt, the CPU cost scales with the square of the number of salt particles and can be orders of magnitude slower than the model presented here. We expect the presented model to be valuable for including proton equilibria in multiscale simulations with many ionizable macromolecules.

Acknowledgment. This work was supported by the Conselho Nacional de Desenvolvimento Científico e Tecnológico (CNPq), Fundação de Amparo à Pesquisa do Estado de São Paulo (FAPESP) and the Swedish Research Council through a Linnaeus grant. We thank CENAPAD-SP for computational resources and, for useful comments, Jan Forsman, Bo Jönsson, and Björn Persson.

References

- (1) Perutz, M. F. Electrostatic Effects in Proteins. *Science* **1978**, *201*, 1187–1191.
- (2) Linse, S.; Johansson, C.; Brodin, P.; Grundström, T.; Drakenberg, T.; Forsén, S. Electrostatic contributions to the binding of Ca^{2+} in calbindin D_{9k} . *Biochemistry* **1991**, *30*, 154–162.

- (3) Woodward, C. E.; Svensson, B. Potentials of mean force in charged systems: Application to Superoxide Dismutase. *J. Phys. Chem.* **1991**, *95*, 7471–7477.
- (4) Foegeding, E. A.; Luck, P.; Davis, J. Factors determining the physical properties of protein foams. *Food Hydrocolloids* **2006**, *20*, 284–292.
- (5) Proctor, V. A.; Cunningham, F. E. The Chemistry of Lysozyme and its use as a Food Preservative and a Pharmaceutical. *CRC Crit. Rev. Food Nutrition* **1988**, *26*, 359–3958.
- (6) Dickinson, E. Interfacial structure and stability of food emulsions as affected by protein-polysaccharide interactions. *Soft Matter* **2008**, *4*, 932–942.
- (7) Biró, E.; Németh, A. S.; Sisak, C.; Feczko, T.; Gyenis, J. Preparation of chitosan particles suitable for enzyme immobilization. *J. Biochem. Biophys. Methods* **2008**, *70*, 1240–1246.
- (8) Saksena, S.; Zydney, A. L. Effect of solution pH and ionic strength on the separation of albumin from immunoglobulins (IgG) by selective filtration. *Biotechnol. Bioeng.* **1994**, *43*, 960–968.
- (9) Wang, Y.-F.; Gao, J. Y.; Dubin, P. L. Protein Separation via Polyelectrolyte Coacervation: Selectivity and Efficiency. *Biotechnol. Prog.* **1996**, *12*, 356–362.
- (10) Wang, Y.; Dubin, P. Protein binding on polyelectrolyte-treated glass. Effect of structure of adsorbed polyelectrolyte. *J. Chromatogr. A* **1998**, *808*, 61–70.
- (11) van Eijndhoven, R. H. C. M.; Saksena, S.; Zydney, A. L. Protein fractionation using electrostatic interactions in membrane filtration. *Biotechnol. Bioeng.* **1995**, *48*, 406–414.
- (12) Lund, M.; Jönsson, B. On the charge regulation of proteins. *Biochemistry* **2005**, *44*, 5722–5727.
- (13) Jönsson, B.; Lund, M.; da Silva, F. L. B. Electrostatics in Macromolecular Solution. In *Food Colloids: Self-Assembly and Material Science*; Dickinson, E., Leser, M. E., Eds.; Royal Society of Chemistry: London, 2007; Vol. 9.
- (14) Da Silva, F. L. B.; Jönsson, B. Polyelectrolyte-protein complexation driven by charge regulation. *Soft Matter* **2009**, *5*, 2862–2868.
- (15) Timasheff, S. N.; Dintzis, H. M.; Kirkwood, J. G.; Coleman, B. D. Studies of molecular interaction in isoionic protein solutions by light-scattering. *Proc. Natl. Acad. Sci. U.S.A.* **1955**, *41*, 710–714.
- (16) Timasheff, S. N.; Dintzis, H. M.; Kirkwood, J. G.; Coleman, B. D. Light Scattering Investigation of Charge Fluctuations in Isoionic Serum Albumin Solutions. *J. Am. Chem. Soc.* **1957**, *79*, 782–791.
- (17) Timasheff, S. N. Specific interactions in proteins due to proton fluctuations. *Biopolymers* **1966**, *4*, 107–120.
- (18) Ståhlberg, J.; Jönsson, B. Influence of Charge Regulation in Electrostatic Interaction Chromatography of Proteins. *Anal. Chem.* **1996**, *68*, 1536–1544.
- (19) Menon, M. K.; Zydney, A. L. Determination of effective protein charge by capillary electrophoresis: effects of charge regulation in the analysis of charge ladders. *Anal. Chem.* **2000**, *72*, 5714–5717.
- (20) da Silva, F. L. B.; Lund, M.; Jönsson, B.; Åkesson, T. On the Complexation of Proteins and Polyelectrolytes. *J. Phys. Chem. B* **2006**, *110*, 4459–4464.
- (21) de Vos, W. M.; Leermakers, F. A. M.; de Keizer, A.; Cohen Stuart, M. A.; Kleijn, J. M. Field Theoretical Analysis of Driving Forces for the Uptake of Proteins by Like-Charged Polyelectrolyte Brushes: Effects of Charge Regulation and Patchiness. *Langmuir* **2010**, *26*, 249–259.
- (22) Linderstrøm-Lang, K. Om proteinstoffernes ionization Compt. *Rend. Trav. Lab. Carlsberg* **1924**, *15*, 1–29.
- (23) Kirkwood, J. G.; Shumaker, J. B. Forces Between Protein Molecules in Solution Arising from Fluctuations in Proton Charge and Configuration. *Proc. Natl. Acad. Sci. U.S.A.* **1952**, *38*, 863–871.
- (24) Netz, R. R. Electrostatics of counter-ions in and between planar charged walls: From Poisson-Boltzmann to the strong-coupling theory. *Eur. Phys. J. E.* **2001**, *5*, 557–574.
- (25) Hill, T. L. *An Introduction to Statistical Thermodynamics*; Dover Publications: Mineola, NY, 1987.
- (26) Evans, D. F.; Wennerström, H. *The Colloidal Domain: Where Physics, Chemistry, Biology, and Technology Meet*; John Wiley & Sons, Ltd.: New York, 1999.
- (27) Holmberg, K.; Jönsson, B.; Kronberg, B.; Lindman, B. *Surfactants and Polymers in Aqueous Solution*, 2nd ed.; John Wiley & Sons, Ltd.: New York, 2002.
- (28) Jönsson, B.; Ullner, M.; Peterson, C.; Sommelius, O.; Söderberg, B. Titrating Polyelectrolytes - Variational Calculations and Monte Carlo Simulations. *J. Phys. Chem.* **1996**, *100*, 409–417.
- (29) Kesvatera, T.; Jönsson, B.; Thulin, E.; Linse, S. Ionization Behavior of Acidic Residues in Calbindin D_{9k}. *Proteins: Struct., Funct., Genet.* **1999**, *37*, 106–115.
- (30) André, I.; Kesvatera, T.; Jönsson, B.; Åerfeldt, K. S.; Linse, S. The Role of Electrostatic Interactions in Calmodulin-Peptide Complex Formation. *Biophys. J.* **2004**, *87*, 1929–1938.
- (31) Labbez, C.; Jönsson, B.; Skarba, M.; Borkovec, M. Ion-Ion Correlation and Charge Reversal at Titrating Solid Interfaces. *Langmuir* **2009**, *25*, 7209–7213.
- (32) Kirkwood, J. G. Theory of Solutions of Molecules Containing Widely Separated Charges with Special Application to Zwitterions. *J. Chem. Phys.* **1934**, *2*, 351–361.
- (33) Tanford, C.; Kirkwood, J. G. Theory of Protein Titration Curves I. General Equations for Impenetrable spheres. *J. Am. Chem. Soc.* **1957**, *79*, 5333–5339.
- (34) Baker, N. A.; Sept, D.; Joseph, S.; Holst, M. J.; McCammon, J. A. Electrostatics of nanosystems: Application to microtubules and the ribosome. *Proc. Natl. Acad. Sci. U.S.A.* **2001**, *98*, 10037–10041.
- (35) Thompson, A.; Boland, M.; Singh, H. *Milk Proteins: From Expression to Food*; Academic Press: New York, 2008.
- (36) Dickinson, E.; Leser, M. E. *Food Colloids: Self-Assembly and Material Science*; Royal Society of Chemistry: London, 2007.
- (37) Gottschalk, M.; Nilsson, H.; Roos, H.; Halle, B. Protein self-association in solution: The bovine β -lactoglobulin dimer and octamer. *Protein Sci.* **2003**, *12*, 2404–2411.
- (38) Fast, J.; Mossberg, A.-K.; Svanborg, C.; Linse, S. Stability of HAMLET - A kinetically trapped α -lactalbumin oleic acid complex. *Protein Sci.* **2005**, *14*, 329–340.
- (39) Chrysina, E.; Brew, K.; Acharya, K. Crystal structures of apo- and holo-bovine alpha-lactalbumin at 2.2-Å resolution reveal an effect of calcium on inter-lobe interactions. *J. Biol. Chem.* **200**, *275*, 37021–37029.

- (40) Brownlow, S.; Morais Cabral, J.; Cooper, R.; Flower, D.; Yewdall, S.; Polikarpov, I.; North, A.; Sawyer, L. Bovine beta-lactoglobulin at 1.8 Å resolution-still an enigmatic lipocalin. *Structure* **1997**, *5*, 481–495.
- (41) Phillies, G. D. J. Excess chemical potential of dilute solutions of spherical polyelectrolytes. *J. Chem. Phys.* **1974**, *60*, 2721–2731.
- (42) Grant, M. L. Nonuniform Charge Effects in Protein-Protein Interactions. *J. Phys. Chem. B* **2001**, *105*, 2858–2863.
- (43) Tanford, C.; Hauenstein, J. D. Hydrogen Ion Equilibria of Ribonuclease. *J. Am. Chem. Soc.* **1956**, *78*, 5287–5291.
- (44) Metropolis, N.; Ulam, S. The Monte Carlo method. *J. Am. Stat. Assoc.* **1949**, *44*, 335–341.
- (45) Allen, M. P.; Tildesley, D. J. *Computer Simulation of Liquids*; Oxford University Press: New York, 1989.
- (46) Frenkel, D.; Smit, B. *Understanding Molecular Simulation*; Academic Press: New York, 2001.
- (47) Ullner, M.; Jönsson, B. A Monte Carlo Study of Titrating Polyelectrolytes in the Presence of Salt. *Macromolecules* **1996**, *29*, 6645–6655.
- (48) Kesvatera, T.; Jönsson, B.; Thulin, E.; Linse, S. Measurement and Modelling of Sequence-specific pK_a Values of Calbindin D_{9k}. *J. Mol. Biol.* **1996**, *259*, 828.
- (49) Persson, B. A.; Lund, M. Association and electrostatic steering of alpha-lactalbumin-lysozyme heterodimers. *Phys. Chem. Chem. Phys.* **2009**, *11*, 8879–8885.
- (50) Nozaki, Y.; Tanford, C. Examination of titration behavior. *Methods Enzymol.* **1967**, *11*, 715–734.
- (51) Lund, M.; Jönsson, B.; Woodward, C. E. Implications of a high dielectric constant in proteins. *J. Chem. Phys.* **2007**, *126*, 225103–225110.
- (52) Jönsson, B.; Svensson, B. *Monte Carlo simulation of ion-protein binding. In Computer Simulation of Biomolecular Systems*, Vol. 2; van Gunsteren, W. F.; Weiner, P. K.; Wilkinson, A., Eds.; ESCOM: Leiden, 1993.
- (53) da Silva, F. L. B.; Jönsson, B.; Penfold, R. A critical investigation of the Tanford-Kirkwood scheme by means of Monte Carlo simulations. *Protein Sci.* **2001**, *10*, 1415–1425.
- (54) de Carvalho, S. J.; Fenley, M. O.; da Silva, F. L. B. Protein-Ion Binding Process on Finite Macromolecular Concentration. A Poisson-Boltzmann and Monte Carlo Study. *J. Phys. Chem. B* **2008**, *112*, 16766–16776.
- (55) Penfold, R.; Warwicker, J.; Jönsson, B. Electrostatic Models for Calcium Binding Proteins. *J. Phys. Chem. B* **1998**, *102*, 8599–8610.
- (56) Warwicker, J. Simplified methods for pK_a and acid pH-dependent stability estimation in proteins: Removing dielectric and counterion boundaries. *Protein Sci.* **1999**, *8*, 418–425.
- (57) Lin, S.-C.; Lee, W. I.; Shurr, J. M. Brownian Motion of Highly Charged Poly(L-lysine). Effects of salt and polyion concentration. *Biopolymers* **1978**, *17*, 1041–1064.
- (58) Schmitz, K. S. *Macro-ion Characterization: From Dilute Solutions to Complex Fluids*; American Chemistry Society: Washington, DC, 1994.
- (59) Kjellander, R.; Ulander, J. Effective ionic charges, permittivity and screening length: dressed ion theory applied to 1:2 electrolyte solutions. *Mol. Phys.* **1996**, *95*, 495–505.
- (60) Beresford-Smith, B.; Chan, D. Y. C. Electrical double-layer interactions in concentrated colloidal systems. *Faraday Discuss. Chem. Soc.* **1983**, *76*, 65–75.
- (61) da Silva, F. L. B.; Linse, S.; Jönsson, B. Binding of Charged Ligands to Macromolecules. Anomalous Salt Dependence. *J. Phys. Chem. B* **2005**, *109*, 2007–2013.
- (62) Dobnikar, J.; Castañeda Priego, R.; Grünberg, H. H. V.; Trizac, E. Testing the relevance of effective interaction potentials between highly-charged colloids in suspension. *New J. Phys.* **2006**, *8*, 277+.
- (63) Lund, M.; Trulsson, M.; Persson, B. Faunus: An object oriented framework for molecular simulation. *Source Code Biol. Med.* **2008**, *3*:1 [doi:10.1186/1751-0473-3-1].
- (64) Jimenez-Flores, R.; Bleck, G. T.; Brown, E. M.; Butler, J. E.; Creamer, L. K.; Hicks, C. L.; Hollar, C. M.; Ng-Kwai-Hang, K. F.; Swaisgood, H. E. Nomenclature of the Proteins of Cows' Milk - Sixth Revision. *J. Dairy Sci.* **2004**, *87*, 1641–1674.
- (65) Shimazaki, K.-I.; Kawaguchi, A.; Sato, T.; Ueda, Y.; Tomimura, T.; Shimamura, S. Analysis of human and bovine milk lactoferrins by rotofor and chromatofocusing. *Int. J. Biochem.* **1993**, *25*, 1653–1658.
- (66) Bezwoda, W. R.; Mansoor, N. Lactoferrin from human breast milk and from neutrophil granulocytes. Comparative studies of isolation, quantitation, characterization and iron binding properties. *Biomed. Chromatogr.* **1989**, *3*, 121–126.
- (67) Steijns, J. M.; van Hooijdonk, A. C. M. Occurrence, structure, biochemical properties and technological characteristics of lactoferrin. *Br. J. Nutr.* **2000**, *84*, 11–17.
- (68) Baker, E.; Baker, H. A structural framework for understanding the multifunctional character of lactoferrin. *Biochimie* **2009**, *91*, 3–10.

CT1003093